Journal of Applied Mathematics and Physics, 2017, 5, 1899-1907
http://www.scirp.org/journal/jamp
ISSN Online: 2327-4379
ISSN Print: 2327-4352

Bifurcation of Parameter-Space and Chaos in Mira 2 Map

Tao Jiang, Zhiyang Yang

School of Information, Beijing Wuzi University, Beijing, China
Email: zyyang@amss.ac.cn, taojiang@amss.ac.cn

How to cite this paper: Jiang, T. and Yang, Z.Y. (2017) Bifurcation of Parameter-Space and Chaos in Mira 2 Map. *Journal of Applied Mathematics and Physics*, **5**, 1899-1907.
https://doi.org/10.4236/jamp.2017.59160

Received: August 4, 2017
Accepted: October 13, 2017
Published: October 16, 2017

Abstract

In this paper, we investigate Mira 2 map in parameter-space (A-B) and obtain some interesting dynamical behaviors. According to the parameter space of Mira 2 map, we take A and B as some groups of values and display complex dynamical behaviors, including period-1, 2, 3, 4, 5, ⋯, 38, ⋯ orbits, Arnold tongues observed in the circle map [7], crisis, some chaotic attractors, period-doubling bifurcation to chaos, quasi-period behaviors to chaos, chaos to quasi-period behaviors, bubble and onset of chaos.

Keywords

Mira 2 Map, Parameter-Space, Arnold Tongues

1. Introduction

Mira first introduced Mira 1 and 2 maps in [1], 1996. And in [2], Styness *et al.* attained a deeper understanding of the phenomenon—a transition from one chaos regime to another chaos regime via crisis—for B falling in the interval $B_c \in [-2.0501226960083, -2.05012267960082]$ (where B_c denotes the critical value of the parameter B) and other parameter $A = -1.5$.

Mira 2 map [1] has the functional form

$$\begin{cases} x_{n+1} = Ax_n + y_n, \\ y_{n+1} x_n^2 + B. \end{cases} \tag{1}$$

where A and B are real.

Though more dynamical behaviors of Mira 2 map (1) had gotten someone's less attention, we studied Mira 2 map and got many interesting dynamical behaviors, such as the conditions of the existence for fold bifurcation, flip bifurcation, Naimark-Sacker bifurcation and chaos in the sense of Marroto of this map in

[3]. In this paper using numerical simulations [4], we obtained the distribution of dynamics in the parameter plane, the maximum Lyapunov exponent [5], fractal dimension [6] and more complex dynamical behaviors, including period-1, 2, 3, 4, 5, ⋯, 38, ⋯ orbits, Arnold tongues observed in the circle map [7], crisis, some chaotic attractors, period-doubling bifurcations to chaos, quasi-period behaviors to chaos, chaos to quasi-period behaviors, bubble, on set of chaos.

The paper is organized as follows. In Section 2, we give the parameter space of dynamical behaviors of Mira 2 map (1) in $(A-B)$ plane. And in Section 3, the numerical simulations bifurcations in $(A-x)$ and $(B-x)$ planes for different values, the computation of maximum Lyapunov exponent corresponding to bifurcation diagram and the phase portraits at neighborhood of critical values are given.

2. Bifurcation in the Parameter-Space

In this section, we give the parameter space of dynamical behaviors of Mira 2 map (1) in $(A-B)$ plane.

In order to show more dynamics of Mira 2 map (1), we take A and B as the parameters and observe the motions of Mira 2 map (1) according to the initial condition $(x_0, y_0) = (0.001, 0.05)$ of Mira 2 map (1). After computing some groups of the value scopes and the length of the grid of A and B , we find that there exist almost all dynamical motion of Mira 2 map (1) for the parameter interval $A \times B = [-2,2] \times [-4,0.5]$ and it takes relatively less time. The parameter-space of Mira 2 map (1) is shown in **Figure 1**. It is an isoperiodic diagram obtained by discretizing the parameter interval $A \times B = [-2,2] \times [-4,0.5]$ in a grid of 800×900 points equally spaced. This corresponds in **Figure 1** to a same resolution in both A and B axes, that is $\Delta A = \Delta B = 0.005$. For each point

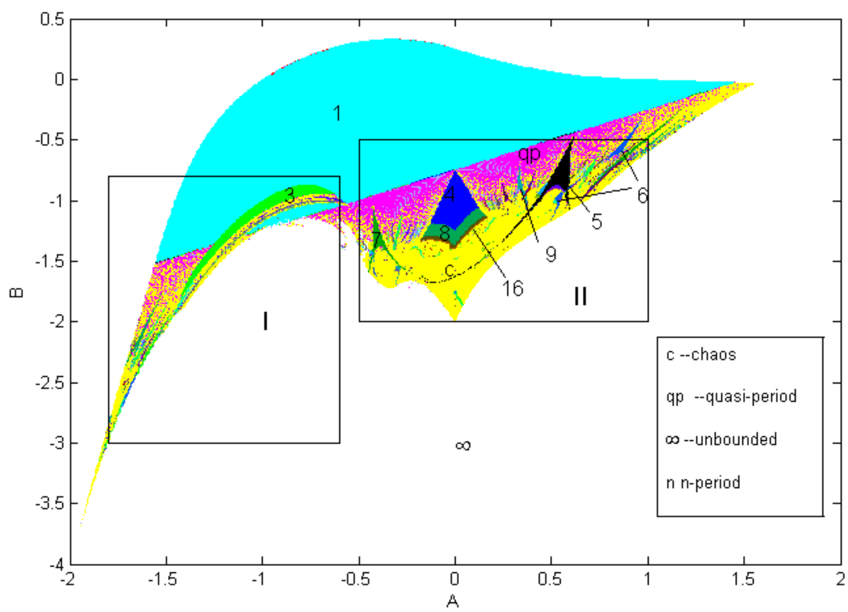

Figure 1. The parameter-space of Mira 2 map (1).

(A,B) in **Figure 1**, an orbit of initial condition $(x_0, y_0) = (0.001, 0.05)$ converges to a chaotic attractor indicated by *c*, or to a quasi-periodic orbit indicated by qp, or to a n-period motion indicated by *n*, or to an attractor in infinity (unbounded attractor) indicated by ∞, after a transient of 5000 iterates.

In **Figure 1**, we can see quasiperiodic motion (purple region) is born exactly on the boundary-the line $B = \frac{A}{2} - \frac{3}{4}$ -of period-1 (cyan) region, as a result of Naimark-Sacker bifurcations of period 1 (we give the condition of the existence of Naimark-Sacker bifurcation in [3]). There is a collection of periodic regions embedded in the quasiperiodic (purple) region not all of these observed clearly with the scale utilized in **Figure 1**. In two plots of **Figure 2** one sees magnifications of the two regions inside of the boxes **I** and **II** of **Figure 1**, the first located in the range $-1.8 \le a \le -0.6, -3 \le b \le -0.8$, and the second in the range $-0.5 \le a \le 1, -2 \le b \le -0.5$. In **Figure 2(a)**, period-1 (cyan) region and period-3 (green) region have well defined boundary. For parameter values taken along the boundary line, pitchfork bifurcation occurs, and parameter *b* decreasing and passing through out period-3 (green) region Naimark-Sacker bifurcation occurs. In **Figure 2(b)**, one sees periodic similar to the Arnold tongues observed immersed in purple region in the circle map [7].

3. Bifurcation and Chaos in Numerical Simulations

Now we present some numerical simulation results to show other interesting dynamical behaviors of Mira 2 map (1). According to the parameter space of Mira 2 map (1) in **Figure 1**, we take A and B as follows:

Case (1). Fixing $A = 0$, and $-2 \le B \le -0.5$;

Case (2). Fixing $A = 0.1$, and $-1.705 \le B \le 0.2$;

Case (3). Fixing $A = 0.5$, and $-1.173 \le B \le -0.4$;

Case (4). Fixing $A = 0.85$, and $-0.785 \le B \le -0.3$;

Case (5). Fixing $B = -2.2$, and $-1.682 \le A \le -1.57$;

For case (1) The bifurcation diagram of Mira 2 map (1) for $A = 0$ in (B, x) plane and the corresponding maximal Lyapunov exponents are given in **Figure 3(a)** and **Figure 3(b)**, respectively. From **Figure 3(a)**, we see period-doubling to

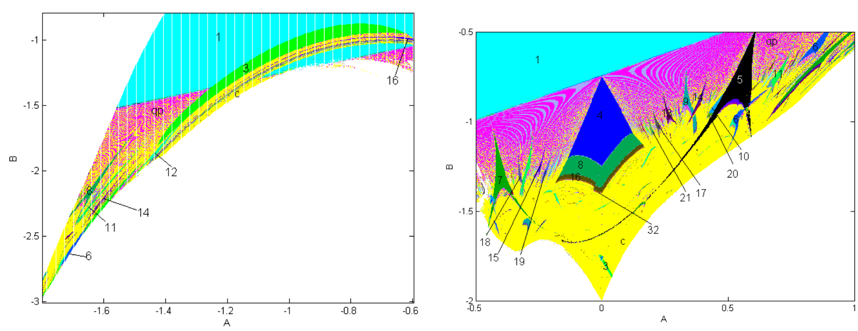

(a) (b)

Figure 2. Magnification of the boxes (a) I, and (b) II in **Figure 1**.

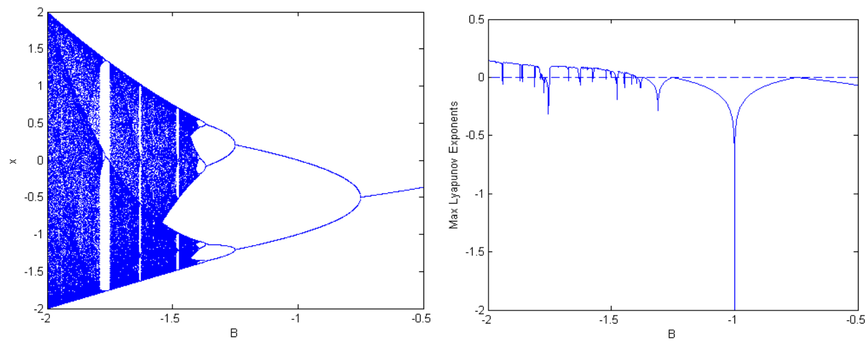

(a) (b)

Figure 3. Bifurcation diagram and Lypunov exponents of Mira 2 map (1). Here $A = 0$.

chaos occur with B decreasing and chaos region abruptly disappears as $B = -1.4746, -1.6243, -1.749$, respectively. And when B decrease to -2, the chaos region turns to an attractor in infinity (unbounded attractor).

For case (2) The bifurcation diagram of Mira 2 map (1) for $A = 0.1$ in (B, x) plane and the corresponding maximal Lyapunov exponents are given in **Figure 4(a)** and **Figure 4(b)**, respectively. In **Figure 4(a)**, Mira 2 map (1) undergoes a Naimark-Sacker bifurcation from period-1 orbit at $B = -0.7$. At B decreasing to $B = -1.0022$, quasi-period region suddenly disappears and six pieces of period-doubling to chaos occur. In the interval $B \in (-1.705, -1.22)$, period-doubling, Naimark-Sacker bifurcation and quasi-period behaviors are immersed in chaos region. The phase portraits of Mira 2 map (1) are shown in **Figures 4(c)-(g)**, respectively. In **Figures 4(c)-(e)**, the size of chaotic attractors at $B = -1.29$ $(\text{MaxLyapunovExponent}(MLE) = 0.0394, \text{FractalDimension}(FD) = 1.4692)$, $B = -1.34(MLE = 0.0559, FD = 2.2151)$, and $B = -1.6(MLE = 0.0836)$, increases with B decreasing. And the quasi-period orbits and its amplification are shown in **Figure 4(f)** and **Figure 4(g)**, respectively.

For case (3) The bifurcation diagram of Mira 2 map (1) for $A = 0.5$ in (B, x) plane and the corresponding maximal Lyapunov exponents are given in **Figure 5(a)** and **Figure 5(b)**, respectively. As B decreasing, Mira 2 map (1) undergoes a Naimark-Sacker bifurcation from period-1 window at $B = \frac{A}{2} - \frac{3}{4} = -0.5$. At $B = -0.8025$, quasi-period region disappears to period-5 windows, and at $B = -0.8915$, period-5 window becomes 15 period-doubling to chaos. **Figures 5(c)-(f)** are shown chaotic attractors at $B = -0.913, (MLE = 0.0106, FD = 1.0723)$, $B = -0.94, (MLE = 0.0269, FD = 1.2055)$, $B = -1, (MLE = 0.045, FD = 1.5670)$ and $B = -1.167(MLE = 0.0845, 1.5278)$, respectively.

For case (4) The bifurcation diagram of Mira 2 map (1) for $A = 0.85$ in (B, x) plane and the corresponding maximal Lyapunov exponents are given in **Figure 6(a)** and **Figure 6(b)**, respectively. And the amplifications of (a) at $-0.665 < B < -0.61$ and $-0.785 < B < -0.68$ are shown in **Figure 6(c)** and

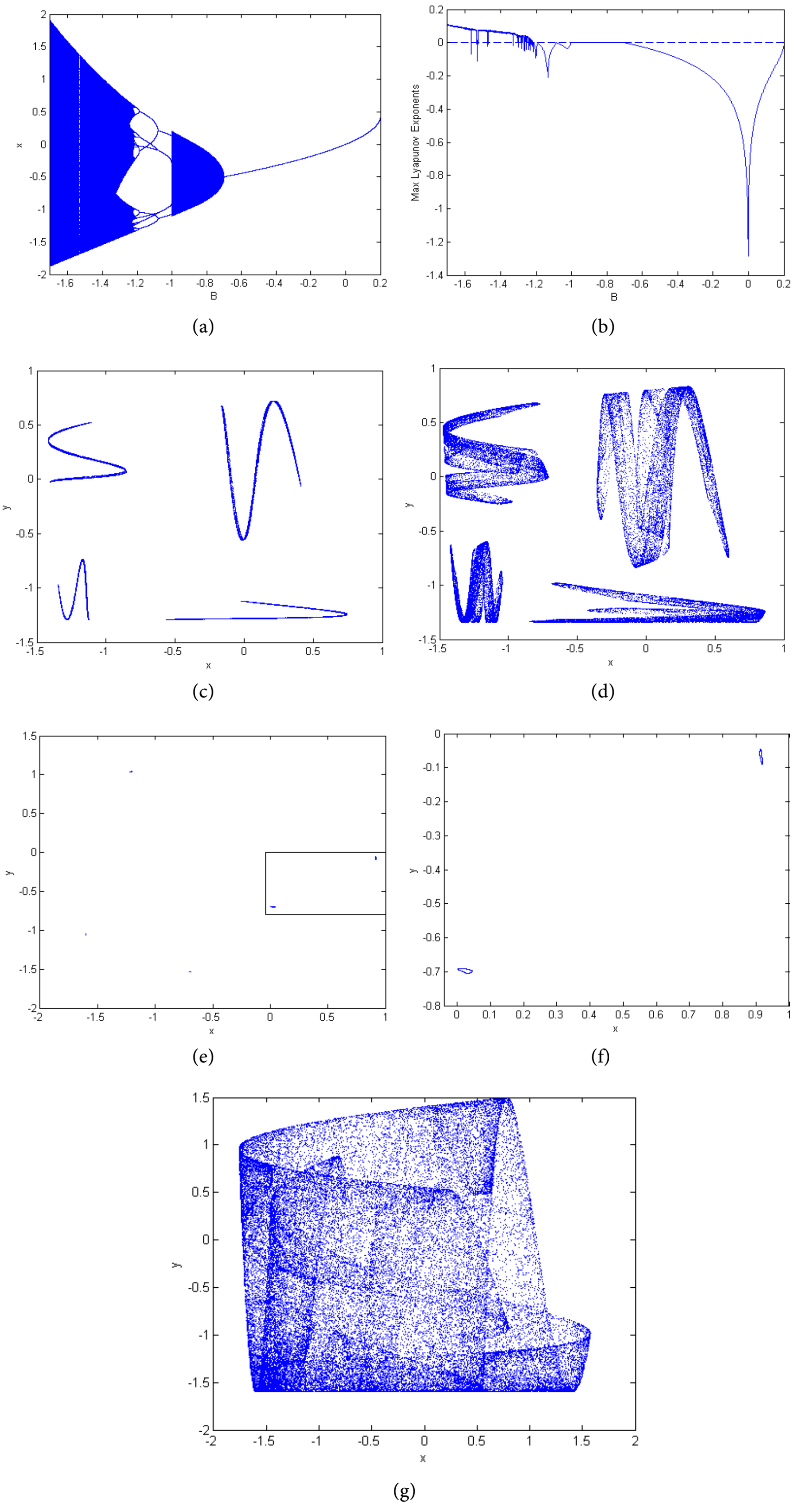

Figure 4. Bifurcation diagram and Lypunov exponents of Mira 2 map (1). Here $A = 0.1$. (c)-(f) Phase portraits of Mira 2 map (1) at $B = -1.29$, $B = -1.34$, $B = -1.6$ and $B = -1.535$. (g) The amplification of (f).

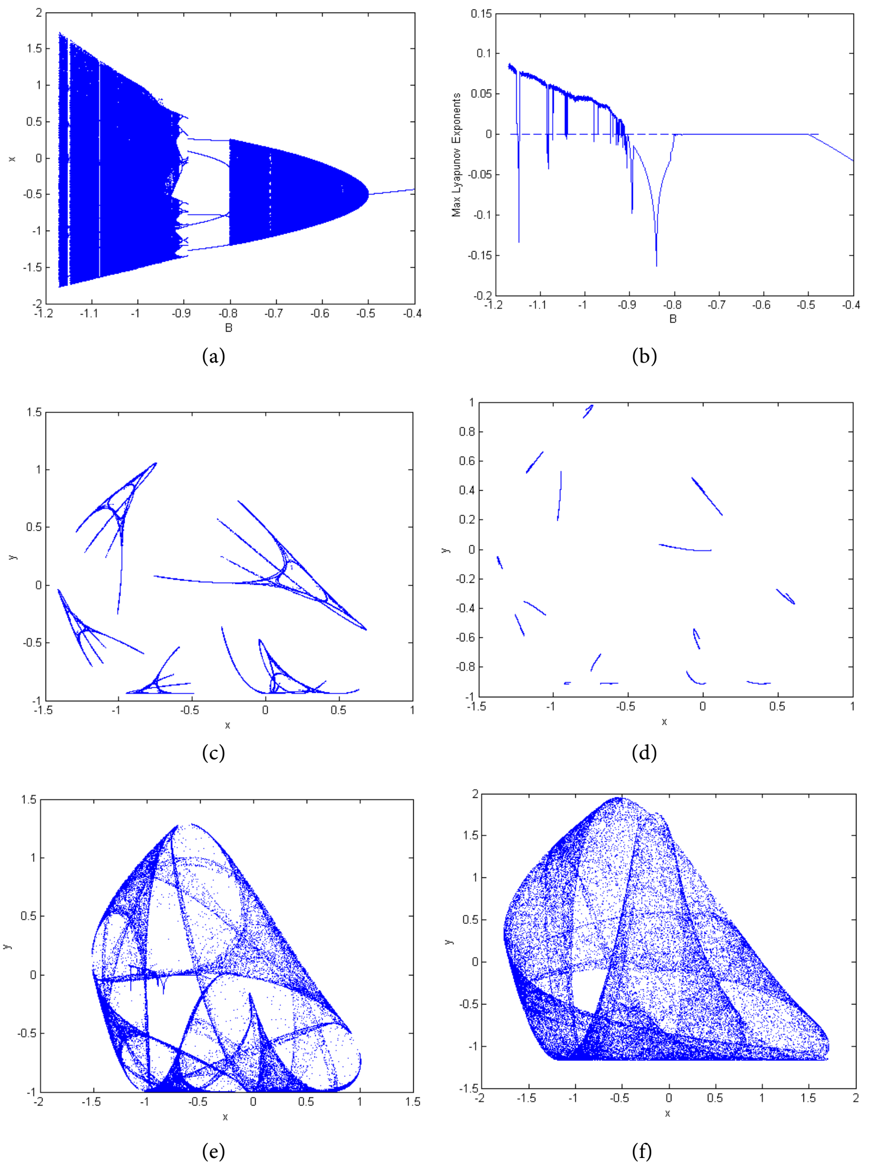

Figure 5. Bifurcation diagram and Lypunov exponents of Mira 2 map (1). Here $A = 0.5$. (c)--(f) Phase portraits of Mira 2 map (1) at $B = -0.913$, $B = -0.94$, $B = -1$ and $B = -1.167$.

Figure 6(d), respectively. In **Figure 6(a)**, Mira 2 map (1) undergoes a Naimark-Sacker bifurcation from period-1 window at $B = A/2 - 3/4 = -0.325$. As B decreasing to $B = 0.5535$, quasi-period behaviors suddenly disappear and period-6 window appears. In **Figure 6(c)**, we observe that quasi-period behaviors and period windows alternatively appear, including period-18, 20, 21, 27, 28, 31, 33, 43, 53, etc. And, as B decreasing to $B = -0.6632$, 7 pieces of inverse period-doubling to chaos appear, and in **Figure 6(d)**, chaos region and period-doubling alternatively appear. The phase portraits of Mira 2 map (1) in **Figures 6(e)-(i)** are chaotic attractors at

$B = -0.6448(MLE = 0.0047, FD = 1.1148)$,

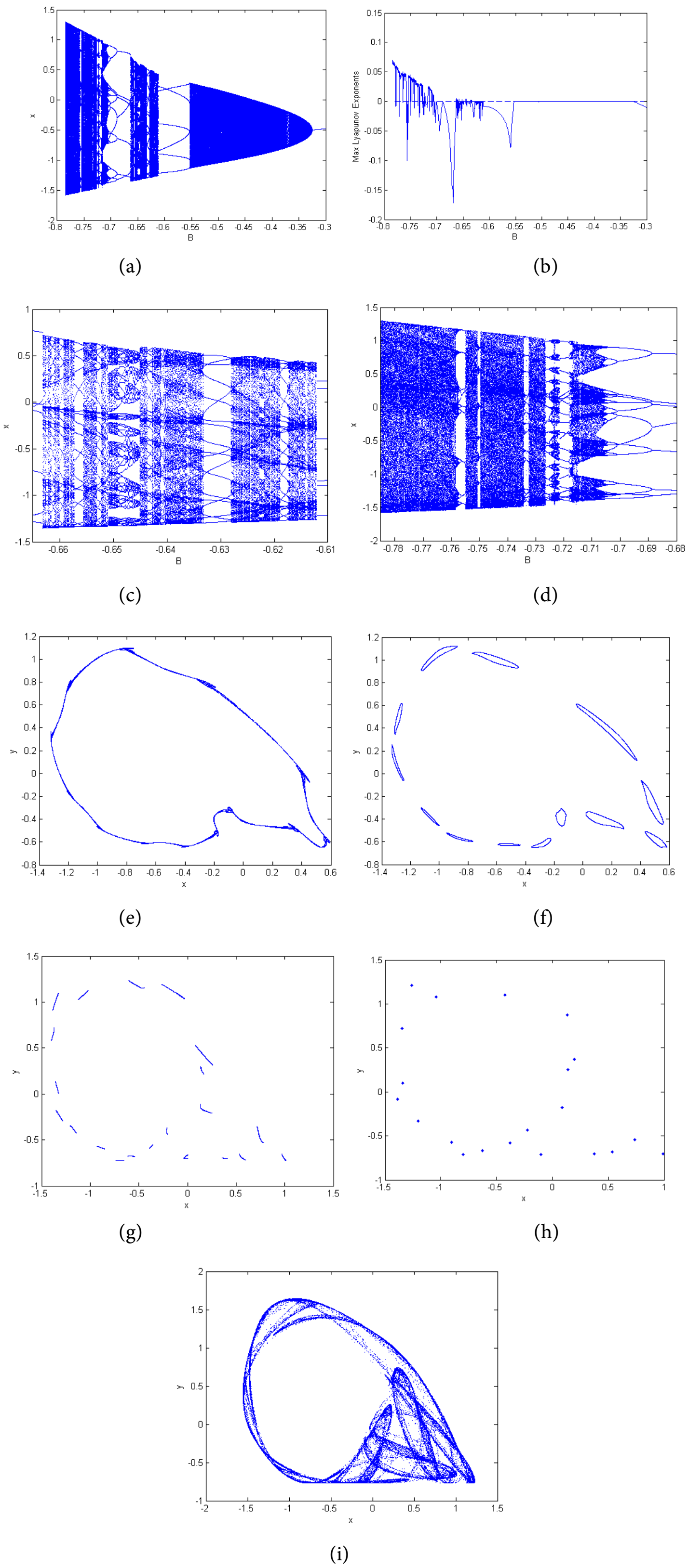

Figure 6. Bifurcation diagram and Lypunov exponents of Mira 2 map (1). Here $A = 0.85$. (c) and (d) The amplification of (a). (e)-(i) Phase portraits of Mira 2 map (1) at $B = -0.6448$, $B = -0.649$, $B = -0.72$, $B = -0.724$ and $B = -0.77$.

$B = -0.724(MLE = 0.007, FD = 1.0815)$ and $B = -0.77(MLE = 0.0423, FD = 1.4178)$, quasi-period orbit at $B = -0.649$, and period-21 orbit at $B = -0.72$, respectively.

For case (5) The bifurcation diagram of Mira 2 map (1) for $B = -2.2$ in (A, x) plane and the corresponding maximal Lyapunov exponents are given in **Figure 7(a)** and **Figure 7(c)**, respectively. As A increasing to $A = -1.682$, the

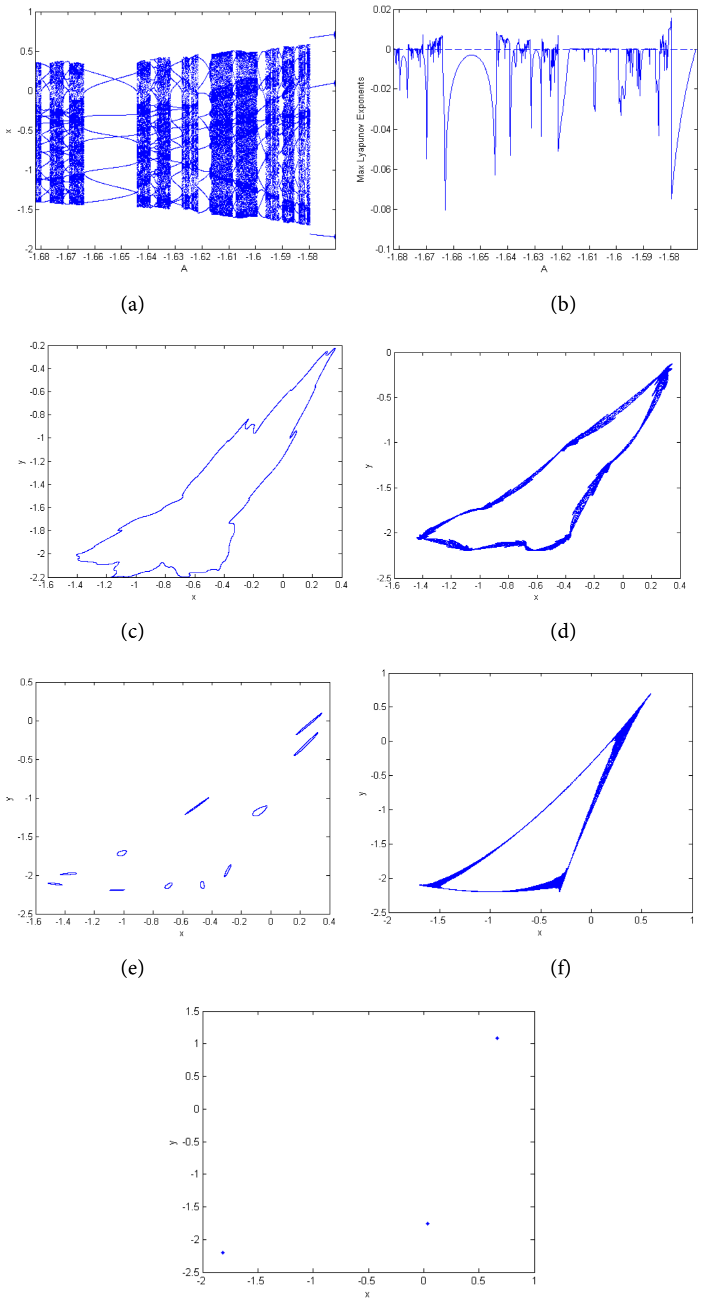

(g)

Figure 7. Bifurcation diagram and Lypunov exponents of Mira 2 map (1). Here $B = -2.2$. (c)-(g) Phase portraits of Mira 2 map (1) at $A = -1.6878$, $A = -1.665$, $A = -1.617$, $A = -1.5798$ and $A = -1.5797$.

attractor in infinity suddenly converges to quasi-period orbit. And as A increasing, quasi-period behaviors, period-orbits which include period-3, 8, 11, 17, 19, 20, 21, 25, etc., and chaotic behaviors alternatively appear. When A increase from $A=-1.5798$ to $A=-1.5797$, chaos disappears and period-3 orbit appear. We observe that 3 pieces of Naimark-Sacker bifurcation occur at $A=-1.5707$. As A increasing to $A=-1.5707$, quasi-period behaviors suddenly disappear and the unbounded attractor appears. The phase portraits of quasi-period orbit, chaotic attractor, period-orbit of Mira 2 map (1) are shown in **Figures 7(c)-(g)** for $A=-1.6878$, $A=-1.665(MLE=0.0057, FD=1.1717)$, $A=-1.617$, $A=-1.5798(MLE=0.016, FD=1.1055)$ and $A=-1.5797$, respectively.

4. Conclusion

In this paper, we study Mira 2 map in parameter-space (A-B) and obtain some interesting dynamical behaviors. According to the parameter space of Mira 2 map, we take A and B as some groups of values and display complex dynamical behaviors.

Acknowledgements

This work was supported by the National Science Foundations of China (10671063 and 61571052).

References

[1] Mira, C., Barugola, A. and Gardini, L. (1996) Chaotic Dynamics in Two-Dimensional Nonvertible Map. World Scientific Publishing, Singapore. https://doi.org/10.1142/2252

[2] Styness, D., Hanan W.G., Pouryahya, S. and Herffernan, D.M. (2010) Scaling Relations and Critical Exponents for Two Dimensional Two Parameter Maps. *The European Physical Journal B*, **77**, 469-478. https://doi.org/10.1140/epjb/e2010-00265-4

[3] Jiang, T. and Yang, Z.Y. (2017) Bifurcations and Chaos in Mira 2 Map. Acta Mathematicae Applicatae Sinica, English Series (Accepted).

[4] Nusse, H.E. and Yorke, J.A. (1997) Dynamics: Numerical Explorations. Springer, New York.

[5] Cartwright, J.H.E. (1999) Nonlinear Stiffness, Lyapunov Exponents, and Attractor Dimension. *Physics Letters A*, **26**, 298-302. https://doi.org/10.1016/S0375-9601(99)00793-8

[6] Agiza, H.N., Elabbssy, E.M., El-Metwally, H. and Elsadany, A.A. (2009) Chaotic Dynamics of a Discrete Prey-Predator Model with Holling Type II. *Nonlinear Analyse*: *Real World Application,* **10**, 116-129. https://doi.org/10.1016/j.nonrwa.2007.08.029

[7] Schuster, H.G. and Just, W. (2005) Deterministic Chaos: An Introduction. 4th Edition, Wiley-VCH Verlag GmbH & Co., Weinheim. https://doi.org/10.1002/3527604804